

Progress on the NML Laser-Cooled Ytterbium Ion Microwave Frequency Standard

Bruce Warrington¹, Peter Fisk, Michael Wouters and Malcolm Lawn

*National Measurement Laboratory, CSIRO Australia
PO Box 218, Lindfield NSW 2070, Sydney, Australia*

Abstract

Microwave frequency standards based on the 12.6 GHz ground state hyperfine ‘clock’ transition in trapped and cooled $^{171}\text{Yb}^+$ ions have been under development at the CSIRO National Measurement Laboratory, in Sydney, Australia, for several years. The first measurement of the clock transition frequency using a laser-cooled ion cloud has been completed. Good agreement is obtained with previous measurements made using a helium buffer gas for cooling, providing an important validation of a complex model used to evaluate the much larger second-order Doppler shift in this case. The present accuracy of 8 parts in 10^{14} is limited solely by technical effects such as the homogeneity of the magnetic field, and the projected uncertainty achievable in a redesigned ion trap is 4 parts in 10^{15} or better. The projected frequency stability is comparable to the exceptional stability already demonstrated using buffer gas cooling $\sigma_y(\tau)=5\times 10^{-14} \tau^{-1/2}$. The performance of a microwave frequency standard based on a cloud of trapped, laser-cooled $^{171}\text{Yb}^+$ ions can therefore be comparable to that of a cesium fountain.

1. Introduction

Microwave frequency standards based on the 12.6 GHz ground-state hyperfine (‘clock’) transition in trapped $^{171}\text{Yb}^+$ ions have demonstrated a stability characterised by a fractional Allan deviation $\sigma_y(\tau) = 5\times 10^{-14} \tau^{-1/2}$ and a frequency uncertainty of ± 1.1 parts in 10^{13} when operated with a He buffer gas for ion cooling [1–3]. The greatest contribution to the frequency uncertainty is the second-order Doppler shift due to the ion thermal motion, which can be reduced by laser cooling the ions to sub-kelvin temperatures.

We have previously reported microwave spectroscopy of laser-cooled $^{171}\text{Yb}^+$ [4], and have also completed an extensive series of measurements of the ion temperature to quantify the remaining second-order Doppler shifts [5]. Here we report a preliminary measurement of the clock transition frequency, based on the first operation of a microwave frequency standard using a laser-cooled ion cloud [6].

A complete evaluation of systematic frequency shifts and associated uncertainties has not yet been completed, but the dominant effects are discussed here. At present, the limiting uncertainty is due to residual magnetic field inhomogeneity associated with the UHV chamber itself. We are currently finalizing a redesign of the UHV chamber in entirely non-magnetic materials. Reasonable projections indicate a performance comparable to that of a cesium fountain, both in frequency stability and in absolute frequency accuracy.

2. Experimental Apparatus

Details of the NML trapped-ion frequency standards have been given previously [1]. The linear Paul trap is shown in Figure 1, and the relevant energy levels and transitions for Yb^+ in Figure 2.

¹ bruce.warrington@csiro.au

The trap operates inside a stainless steel UHV chamber (base pressure below 1×10^{-8} Pa) surrounded by four layers of magnetic shielding. The ambient magnetic field is controlled using three-axis Helmholtz coils, and additional coils compensate for residual gradients.

The resonance transition near 369 nm is used for laser cooling, and to prepare and probe the populations of the ground state levels; this light is generated by a Coherent frequency-doubled titanium-doped sapphire laser. A small fraction of the ions decay to the metastable $^2D_{3/2}$ level; the transition at 609 nm returns these ions to the cooling cycle, using light generated by a Spectra-Physics 380D dye laser. Finally, the transition between the ground state hyperfine levels is the reference frequency for the standard. Microwave radiation near 12 642 812 120 Hz for spectroscopy of this transition is synthesized from a sapphire-loaded superconducting dielectric resonator oscillator [7]. This radiation is also applied during cooling, in order to drain population accumulating in the lower hyperfine level.

Following loading, the RF and DC potentials of the linear trap are reduced for laser cooling. The fluorescence decreases sharply as the cloud approaches its coldest temperature, but it is likely that this ‘phase transition’ is to a liquid-like rather than a crystalline state [8]: we calculate a Coulomb coupling parameter (the ratio of electrostatic potential energy to thermal energy $k_B T$) of $\eta \sim 0.5$ at $T = 0.4$ K, well below the transition value observed for large ion crystals [9]. After cooling, the RF frequency Ω is increased from 500 kHz to 750 kHz; this appears necessary to minimise the rate at which the ion cloud heats, although the reason is not fully understood.

3. Measurement of the Transition Frequency

Spectroscopy of the $M_F = 0 \rightarrow 0$ ‘clock’ hyperfine component of the 12.6 GHz transition uses Ramsey’s method, with two $\pi/2$ pulses of length $t = 400$ ms separated by $t_R = 10$ s between pulse centres. The 369 nm light is blocked during the interrogation sequence to prevent light shifts, then reapplied to record the ion fluorescence as a measure of the microwave absorption. The ion cloud is subsequently recooled for 2 s, with the microwave field switched off for the last part of the cooling to prepare the ions in the lower hyperfine state for the next interrogation. The microwave frequency is adjusted to match the ion transition by recording fluorescence at the half-height points of the central fringe. The ambient magnetic field is determined from the Larmor frequency ν , obtained by similarly tracking the $M_F = 0 \rightarrow -1$ Zeeman component using Ramsey pulses with $t = 1$ ms and $t_R = 2$ ms. A measurement cycle consists of a frequency measurement (two count periods) for both the clock and Zeeman components, with a cycle time of 38 s. Data presented here were collected with a cloud of radius $r = 0.85$ mm over two hours.

The absolute frequency calibration of the applied microwave field is conducted in two stages. A 2.88 GHz frequency signal derived from the sapphire resonator is directly compared to a similar signal from a hydrogen maser, which must then be separately compared to the SI second. Since the only local cesium references are commercial beam standards with insufficient frequency accuracy, the calibration must be made by common-view GPS frequency transfer. The corresponding uncertainty (5 parts in 10^{14}) is at present comparable to that associated with other systematic effects discussed below, but more precise methods will be required once the systematic uncertainty in the frequency measurements reaches projected levels.

4. Systematic Shifts

Values for the dominant systematic frequency offsets are given in Table 1 (reproduced from Ref. [6]).

Second-order Doppler shifts are associated with both the driven (micromotion) and free (secular) components of the ion motion in the usual pseudopotential approximation. The micromotion component may be readily calculated [6], with a mean shift for the ion cloud proportional to the square of the cloud radius r . We obtain a shift of approximately $(6\pm 2)\times 10^{-15}$ for an ellipsoid with $r=1$ mm, where the uncertainty is conservative. This is of the same order as or smaller than the collisional shift in a cesium fountain. The shift associated with thermal motion must be characterized separately by measuring the kinetic energy of secular motion, or equivalently the effective secular temperature obtained from the lineshape of the resonance transition [5]. Although this temperature rises during the microwave interrogation since the cooling light must be blocked to prevent light shifts, the corresponding second-order Doppler shift remains below 1×10^{-15} for Ramsey intervals t_R up to 10 s and beyond (see Figure 3).

The second-order Zeeman shift is obtained from the Larmor frequency ν using standard expressions. The uncertainty Δ in this correction scales as the product $\nu\cdot\delta\nu$, where the uncertainty $\delta\nu$ is conservatively taken to be the FWHM of the Zeeman component pending a more detailed investigation of the lineshape. For the data presented here, $\nu\sim 17$ kHz, $\delta\nu\sim 75$ Hz and $\Delta=3\times 10^{-14}$. An effort was made to minimise magnetic field gradients (and consequently $\delta\nu$) using compensation coils, and subsequent optimization has improved the minimum uncertainty by an order of magnitude to $\Delta=2\times 10^{-15}$ (see Figure 4). However, we believe that the homogeneity of the magnetic field is presently limited by unavoidable stray fields associated with the stainless steel UHV chamber.

Other systematic shifts listed in Table 1 have been evaluated using standard expressions and additional experimental data [6] and are essentially negligible at present. Some additional work may be required to minimize and quantify shifts associated with sidebands and switching transients in the microwave field below the current uncertainty of 3×10^{-15} .

5. Design aspects

Before presenting final results, we note that engineering aspects of the frequency standard are currently being refined in two main areas. Firstly, we are redesigning the UHV system to provide an entirely non-magnetic chamber, for example constructed from Ti, Al, or Cu or their alloys, to provide a homogeneous magnetic field environment at the site of the ion cloud. This should enable us to reliably obtain an uncertainty in the second-order Zeeman shift of 1×10^{-15} or lower. Secondly, although laser-diode-based sources for 369 nm radiation have already been developed, to date they have employed frequency doubling of 740 nm light and are consequently limited to an output power of only 20–30 μ W which is insufficient to cool the ion cloud. However, semiconductor laser diode sources which emit in the near UV at the fundamental have become available relatively recently [10], and we are exploring the possibility that these sources will allow the laser-cooled standard to operate continuously.

6. Results and projected performance

We obtain 12 642 812 118.468 5(7)(6) Hz for the clock transition frequency. The first uncertainty given represents statistical and systematic uncertainties combined in quadrature, at present dominated by corrections for the second-order Zeeman shift and for magnetic field inhomogeneity, and the second refers to the calibration of the hydrogen maser with respect to the SI second. The result is in excellent agreement with measurements obtained for buffer-gas

cooled ions (see Figure 5). Note that the magnitude of the shifts is significantly different in the laser-cooled case: both the second-order Doppler shift and the quadratic Stark shift are smaller by orders of magnitude, and the pressure shift due to the He buffer gas is absent.

The maximum achievable stability for a frequency standard based on laser-cooled $^{171}\text{Yb}^+$ ions is predicted to be better than $\sigma_y(\tau) = 5 \times 10^{-14} \tau^{-1/2}$, which is comparable to the NML buffer-gas cooled standard. This prediction assumes a cloud of radius 1 mm and length 10 mm containing approximately 10^4 ions, a Ramsey pulse separation of 10 s, and a cycle time of 13 s after allowing for cooling periods. The uncertainty budget given in Table 1 indicates no serious obstacle to realising a projected uncertainty of 4×10^{-15} or lower, as systematic shifts associated with the microwave radiation and the homogeneity of the magnetic field have been characterised to an uncertainty well below this level in other standards. Based on these estimates, a cloud of laser-cooled $^{171}\text{Yb}^+$ ions in a linear trap is projected to exhibit comparable performance to a cesium fountain, and continues to show significant promise as a frequency standard of both high accuracy and high stability.

Acknowledgments

The authors thank Dr A. G. Mann and Dr D. G. Blair of the Department of Physics, University of Western Australia, for the loan of the cryogenic sapphire resonator, and Dr P. Hannaford of CSIRO Division of Manufacturing Science and Technology, Melbourne, Australia, for the loan of the dye laser. They would also like to acknowledge the contribution of Mr Colin Coles in electronic and microwave engineering for the ion traps.

References

- [1] Fisk, P. T. H., Sellars, M. J., Lawn, M. A. and Coles, C., 1997, *IEEE Trans. Ultrasonics, Ferroelectrics and Frequency Control*, **44**, 344–354.
- [2] Fisk, P. T. H., Lawn, M. A. and Coles, C., 1997, *Proc. Workshop on the Scientific Applications of Clocks in Space*, NASA Jet Propulsion Laboratory Publication **97-15**, 143–152.
- [3] Fisk P. T. H., Sellars M. J., Lawn M. A. and Coles C., 1996, *Proc. Fifth Symposium on Frequency Standards and Metrology* (World Scientific), 27–32.
- [4] Warrington, R. B., Fisk, P. T. H., Wouters, M. J., Lawn, M. A. and Coles, C., 1999, *Proc. 1999 Joint Meeting EFTF and IEEE FCS*, IEEE **99CH36313**, 125–128.
- [5] Warrington R. B., Fisk P. T. H., Wouters M. J. and Lawn M. A., 2002, *IEEE Trans. Ultrason. Ferroelectr. Freq. Control*.
- [6] Warrington R. B., Fisk P. T. H., Wouters M. J. and Lawn M. A., 2002, *Proc. Sixth Symposium on Frequency Standards and Metrology*.
- [7] Giles A. J. *et al.*, 1990, *Physica B*, **165**, 145–6.
- [8] Turner L, 1987, *Phys. Fluids*, **30**, 3196–3203.
- [9] Drewsen M. *et al.*, 1998, *Phys. Rev. Lett.*, **81**, 2878–81.
- [10] Nichia Corporation, www.nichia.co.jp, part number NDHU200APAE2.
- [11] Tamm Ch., Schnier D. and Bauch A., 1995, *Appl. Phys. B*, **60**, 19–29.
- [12] Sellars M. J., Fisk P. T. H., Lawn M. A. and Coles C., 1995, *Proc. 1995 IEEE Frequency Control Symposium*, 66–73.

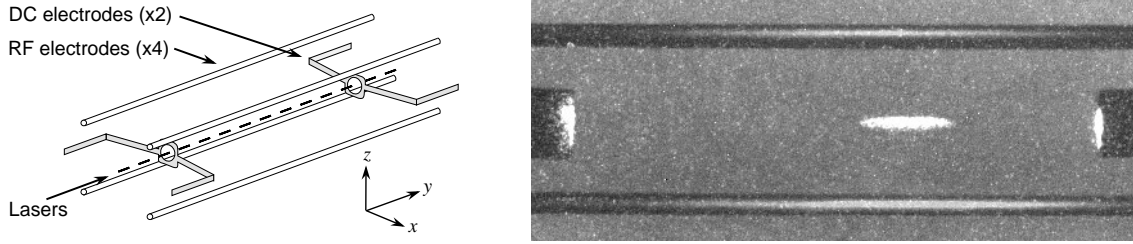


Figure 1: (Left) Electrode configuration of the linear trap. (Right) The laser-cooled ion cloud, approximately 10 mm long with a radius of 1.5 mm. RF electrodes are visible top and bottom (diameter 2.3 mm, separation 20 mm) and DC electrodes left and right (separation 60 mm).

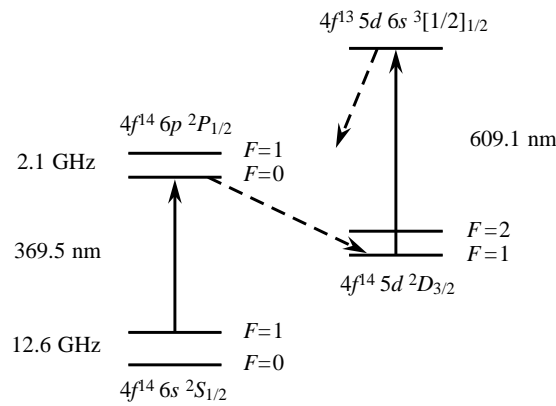


Figure 2: Partial energy level diagram of the $^{171}\text{Yb}^+$ ion.

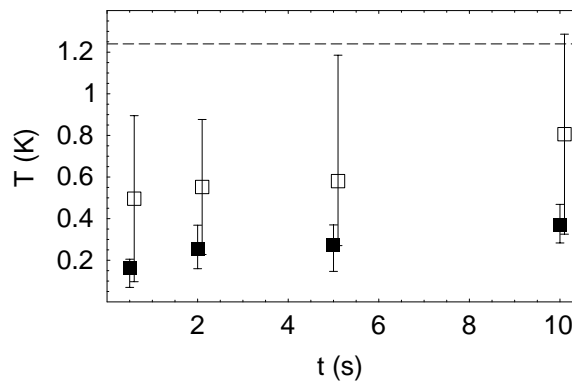


Figure 3: Effective temperature T for a typical ion cloud as a function of time t for which the cooling light has been blocked, for secular motion along the trap symmetry axis (solid) and transverse to this axis (open) [5]. Data not presented here indicate that the apparent excess in transverse temperature is consistent with an experimental artefact, and thus that the cloud is sufficiently close to thermal equilibrium. The dashed line marks the temperature corresponding to a fractional second-order Doppler shift of 1×10^{-15} .

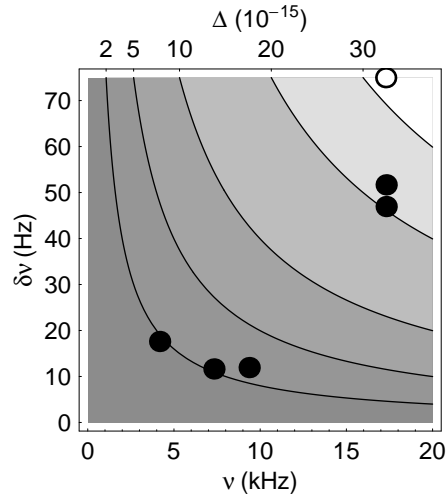


Figure 4: Uncertainty Δ in the second-order Zeeman correction as a function of Larmor frequency ν and its uncertainty $\delta\nu$ obtained from the FWHM of the Zeeman component. The open point corresponds to the frequency measurement reported here, and the closed points to subsequent optimizations of the homogeneity of the applied magnetic field.

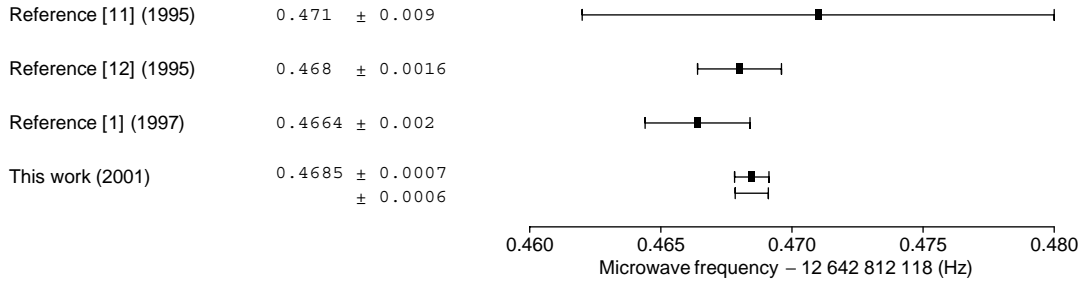


Figure 5: Recent measurements of the clock transition frequency. Separate error bars for this preliminary measurement show statistical and systematic uncertainties (upper) and the calibration uncertainty for the hydrogen maser (lower).

Shift	Magnitude (10^{-15})		Uncertainty (10^{-15})	
	Present	Projected	Present	Projected
Second-order Zeeman (DC)	<i>3500</i>	500	30	2
Second-order Zeeman (AC, Ω)	<2	<2	2	<1
Magnetic inhomogeneity	<i>40</i>	<2	40	1
Second-order Doppler (micromotion)	4	<10	1	<2
Second-order Doppler (secular)	<1	<1	<1	<1
Quadratic Stark	0.1	<0.5	0.05	<0.2
Blackbody radiation	1.4	1.4	<1	<1
Microwave imperfections	<3	1	<3	1
Pressure shift	<0.5	<0.5	<0.5	<0.5
Combined			50	≤ 4

Table 1. Systematic shifts in the clock transition frequency [6] relative to that of an unperturbed ion at rest. Present and projected values are shown; no correction is applied where only an upper limit on the shift has been evaluated. Values in italics show where further work is required to reach projected performance.